

Calibration of Seismographic Stations for Improved Earthquake Location in 43 States

Grant 06HQGR0106

PI: Paul G. Richards

Lamont-Doherty Earth Observatory of Columbia University, Palisades, NY 10964

Tel: (845) 365 8389; Fax (845) 365 8150; richards@LDEO.columbia.edu

URL: <http://www.LDEO.columbia.edu/~richards>

NEHRP Element III

Keywords: Seismology, Source characteristics

Final Report

This report covers our activities for the two calendar years of funding for this project, 2006 and 2007. The work was done by five scientists at Lamont, namely Won-Young Kim, Bill Menke, Paul Richards (Principal Investigator), David Schaff, and Felix Waldhauser. The goal of this project was to improve procedures that NEIC could use for locating seismic events occurring in 40 states East of the meridian 110°W, plus parts of Idaho, Arizona, and Nevada (eastern part of the craton). The research was based on the development of travel time information, for seismic waves, that is needed separately for each station used by NEIC, in order to interpret the observed arrival times of seismic signals, and thus to estimate locations in this region.

Overview of our investigations

During this two-year project, we began by engaging in two somewhat separate research activities that came together in the third and final stage of the project. First, we developed a 3D model of the crust and upper mantle beneath North America, for which we could quickly compute travel times between any two points. Such travel times were regarded in practice as a sum of two terms, namely: the travel time as calculated for a standard Earth model, plus a correction term, resulting from the differences between our 3D model and the standard model. Second, we developed a list of seismic events, called ground truth or GT events, for which we had confidence that the actual hypocenters were known to within about 5 km. For these so-called GT5 events (or GT10 in some cases, or GT2...) we acquired travel time data and determined the station set for which we needed travel time corrections.

The first of these activities was by far the most labor-intensive component of the whole project. As described further, below, we combined information from extensive surface wave studies and body wave studies, and in particular we developed a 3D model called *NETTLESAK135G* that very significantly improved upon the standard Earth model *ak135* of Kennett et al (1995), in its fit to observed travel times from a series of chemical and nuclear explosions whose signals have been

reported from hundreds of stations across the continental US and parts of Canada. These particular seismic sources have locations known to within 1 km or better (hence, are called GT1 events, and in some cases are GT0) and also have accurate origin times, measured or derived from special information obtained for each source by the organizations that carried out the explosions. The combined dataset of first-arriving *P*-wave travel times from these events is an important component of our research, and is likely to find future uses in the development of better 3D models for North America.

In the second activity we began with the set of 16 GT5 events listed in our proposal. This was expanded to a set of 29 events during the project. We gathered the travel time picks for these events and determined the set of stations for which we needed travel time corrections based on our 3D Earth model *NETTLESAK135G*. We computed these corrections for a grid of half-degree by half-degree source locations. At the final stage of our work, when we began relocation of these events using a variety of travel time models, and compared the resulting locations with the PDE and GT locations, we made a few changes in our event selection.

In the third and final stage of the project, in order to make our own location estimates we applied the LOCSAT code developed over a period of several years for operational use in data centers that analyze seismic signals to monitor for nuclear explosions. Of course most of the events located by such centers are earthquakes. This code can accept data of three types, namely slowness (S), azimuth (A), and travel time (T), hence its name. Slowness and azimuth can be measured by arrays. In this project we used travel time data from numerous single stations, not from any arrays, hence our input data consisted only of travel times.

In sections below, we describe:

- (1) our development of the 3D Earth model *NETTLESAK135G* and the dataset of travel times from GT1 and GT0 events, all of them explosions, used to validate it (this section also describes our approach to computing travel times);
- (2) our choice of GT5 events and a summary of the reasons we consider our GT information to be of high quality; and
- (3) the preliminary results of various relocation estimates, and their performance for particular events.

About 95% of the effort into this project went into the stages (1) and (2) described above. Although the funding period for this project is now over, and this is our formal final report, we welcome opportunities to continue to work with NEIC/USGS personnel to augment the work we have done so far in stage (3). It will be very helpful to conduct joint work, in order for our location estimates for specific events — based upon our general approach to quantifying the effects of 3D structure, and upon details of our methods — to be compared to location estimates used in current operational procedures at NEIC. Some of the assumptions built into operational procedures, and decisions about what data are selected (or left out), and how the data are weighted, are unknown to us.

In other sections below we give a non-technical summary, a report on presentations we have made during this work, and a description of datasets that are available as a result of this project. A final section comments upon the project as a whole.

Description of our 3D Earth model, and its fit to a travel time dataset

Our principal initial effort, during the first four months of 2006, was the successful adaptation of Menke's code, called "raytrace3d", to the scale of the problem of modeling regional travel times for P_g , P_n , and teleseismic P for sources and stations within North America. In particular, for the region between 23°N to 50°N and 60°W to 125°W, which includes Bermuda, and extending down 1000 km from the Earth's surface, this code was applied to 600,000 tetrahedral cells that were used, first, in a check to see how well the known travel times of the specified *ak135* Earth model can be reproduced; and second, to establish the adaptation to an elliptical Earth model version of *ak135*, with station locations and source locations specified via geographic rather than geocentric latitudes. The way we think of each tetrahedral cell is illustrated in Figure 1.

Choice of linear splines and tetrahedra motivated by **efficiency**

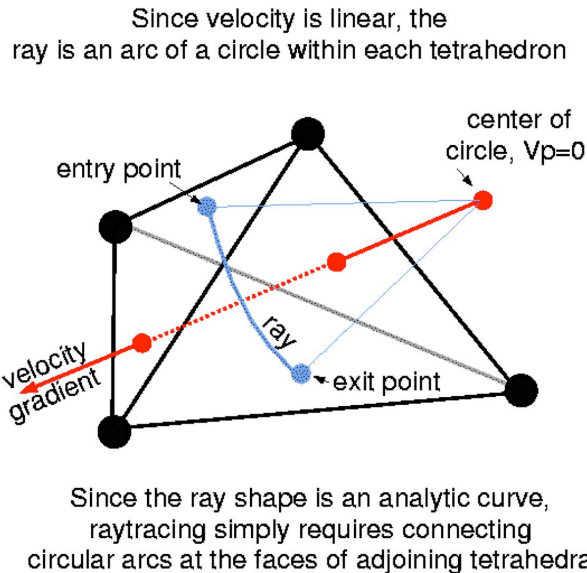


Figure 1. In each cell, there is a constant seismic velocity gradient and the ray path is an arc of a circle. The whole ray path from source to station is a succession of arcs.

The precision of *ak135* travel times obtained with this code was much smaller (i.e. much better) than the effects of ellipticity, which could be accommodated routinely though it has a smaller effect on travel times than the path corrections which are our main interest. Taking the lateral spacing of nodes as 0.25° brought the number of cells up to about two million, and presented no difficulty. The Beowulf Linux cluster at Lamont allows computation for up to about ten million cells.

Although the raytrace3d code, based upon a cartesian coordinate system, could be used for global models, it was not well suited to them. Menke therefore developed a new code named "raytracese" specifically for this project, that facilitated computation in elliptical Earth models. This code too represents the Earth as a collection of tetrahedra, with properties such as compressional velocity specified at the vertices of the tetrahedra, and with linear interpolation used to define values inside each tetrahedron. Raytracing is accomplished by the following three-step "shooting" process:

- Step 1, a database of ray-pencils is computed, all with a common source but a suite of azimuths and angles of incidence;
- Step 2: This database is queried to determine all ray-pencils that enclose a given receiver, thus yielding an estimate of the take-off parameters for all rays arriving at the receiver; and
- Step 3: Take-off parameters are iteratively refined using Newton's method, in order to find a particular ray that fits between the source and the target station.

The accuracy of this travel-time calculation was tested in two ways:

- 1) Travel times for a surface source in a spherical *AK135* *P*-wave model made up of tetrahedrons was compared directly against published *ak135* traveltimes, for distances < 30 degrees. They agreed to within 1-2 ms, including secondary transition zone arrivals.
- 2) Travel times for an elliptical *AK135* *P*-wave model, a particular station in Colorado and sources on two linear arrays crossing North America (one north-south, one east-west, intersecting near the station) were compared to the output of the LOCSAT earthquake location code, which uses *ak135* and which implements an ellipticity correction. Travel times matched to within 10 ms for epicentral ranges < 25 degrees, but systematically increased at greater ranges (up to 600 ms at 35 deg). The reason for this discrepancy was not determined, but may reflect different assumptions on the ellipticity of transition zone interfaces.

Figure 2 shows a slice through a 3D model of the crust and upper mantle. Figure 3 shows rays in this model.

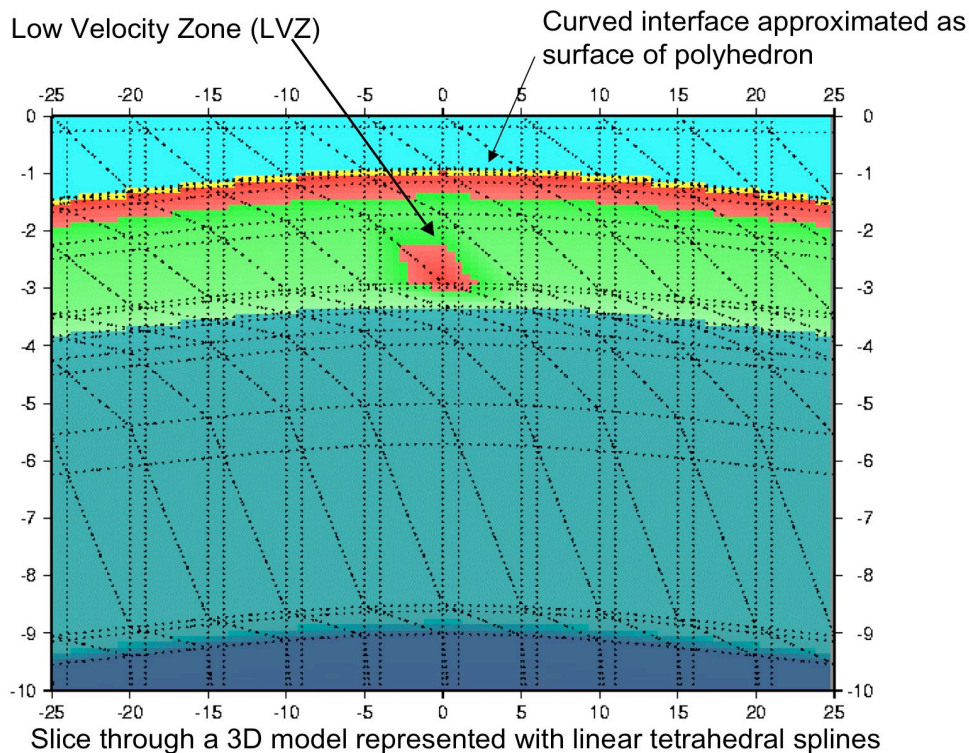
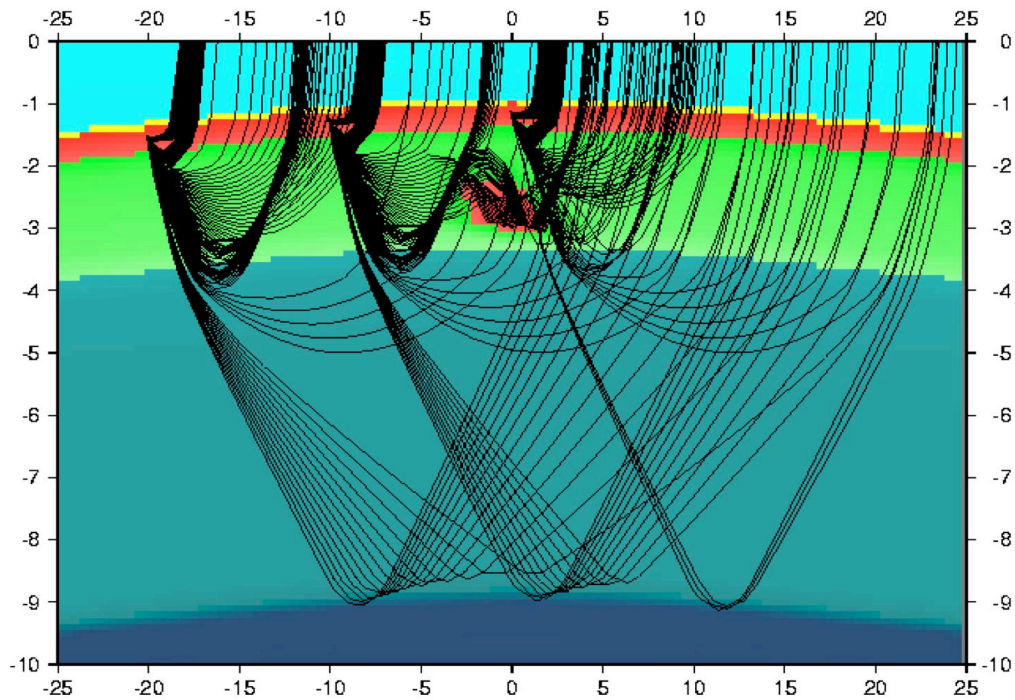


Figure 2

The actual calculation of Source Specific Station Corrections for a particular 3D Earth model reverses the sense of source and receiver. That is, travel times are calculated by shooting rays from a station to a 1/2 degree by 1/2 degree grid of sources distributed over the surface of the earth model. Either one arrival, or several, or none, are possible for each source point (the zero-arrival case represents a shadow zone).



Some sample ray paths

Figure 3. Rays in the slice shown in Figure 2.

These tabulated data are used to create a grid of first arrivals. Unfortunately, simple selection of the first arrival at each source point proved to produce a poor result, owing to occasionally missed arrivals (say, due to a small shadow) at a small percentage of source points. These 'holes' in one of the travel time branches lead to spikes in the resulting map of first arrival travel times. The following, more complicated procedure was developed to eliminate these spikes.

The turning depth of each ray was tabulated along with its travel time, thus allowing travel times to be divided into distinct branches based upon the depth range in which the corresponding ray turned. A grid of each travel time branch was constructed, and bilinear interpolation was used to fill in any 'holes', where a hole was defined to be any unpopulated grid point surrounded by enough populated ones to allow the interpolation to be performed (three, as long as they are not on a straight line).

A single first-arrival travel time grid was then created by merging the data from each travel time

branch, selecting always the earliest arriving one. The resulting grid typically has a few remaining small holes. These holes were then filled using the GMT routine, “surface”, an implementation of interpolation by cubic splines under tension.

About 1.25 hours of CPU time are required for computing a map of first arrival travel times for a single station (and as discussed below we finally needed to work with 429 stations). Twice that time is required to compute a map of differential traveltimes (that is, the difference between two Earth models). All Earth models used tetrahedra organized into sets of layers, whose surfaces paralleled those of the elliptical Earth. The node spacing on these surfaces was always held to 1/2 deg in both latitude and longitude. Only the portion of the Earth bounded by latitudes 26°N and 56°N, longitudes 130°W and 60°W and depths -20 km and 1502.5 km were modeled.

We developed the following Earth models:

AK135: This is the published version of *ak135*, modified in the following ways:

- 1) The published version of *ak135* has a crust consisting of two constant-velocity layers. We replaced this crust with two constant-velocity-gradient layers of the same thickness, with the top, middle and bottom velocities being adjusted so that the overall velocity profile is continuous and 'best fits' the travel times of the constant-velocity layers.
- 2) Our model is explicitly elliptical. We assume that the ellipticity of the transition zone interfaces is the same as that of the earth's surface. The published *ak135* ellipticity corrections do not specify what corresponding ellipticity-depth model was used for their calculation, so our assumed ellipticity may not match the original. However, we believe that the difference is likely to lead to only minor differences in travel time.

NETTLESAK135G: This is based on the published version of the Nettles and Dziewonski (2008) Voigt-averaged shear-wave velocity, V_s , which was mapped to P velocity using a procedure described below. Like many continental-scale surface-wave models, the Nettles and Dziewonski model contains strong negative dV_s/dz velocity gradients that cause large shadow zones in the 5-15 deg range. Figure 4 illustrates this difficulty, which is an important issue, as yet unresolved, in modern geophysics: models of upper mantle structure determined from surface-wave studies have shear velocity V_s decreasing so strongly with depth that they lead to shadow zones which would prohibit the types of body-wave signals we see routinely.

At this point, it is appropriate to give a short description of the methods used by Nettles, in her Ph. D. thesis, to derive a shear-velocity model of the upper mantle beneath North America. This model, given in detail in Nettles and Dziewonski (2008), was developed in a two step process, beginning with acquisition of a surface-wave dispersion dataset of unprecedented size. Love and Rayleigh wave phase-velocity maps for periods in the range 35-150 s were determined in the first step. The second step was to develop a three-dimensional radially anisotropic shear-velocity model of the upper mantle. Nettles' model, which quantifies variations in velocity on a length scale of a few hundred kilometers within the North American continent, was determined together with a longer-wavelength model of the upper mantle for the remainder of the globe. This approach addressed the fact that conventional methods had failed to give an adequate treatment of the peripheral regions of the continent. (Most of the earthquakes needed for tomographic imaging lie outside North America, and the surface waves spreading from these earthquakes have been already distorted by global structure before they cross the continent under the denser network. These distortions in the incident waves had to be studied and corrected for, prior to interpreting the distortions arising from propagation across North America in terms of North American structure.) She found that variations in isotropic velocity in the uppermost several hundred kilometers of the

mantle correlate well with surface tectonic features. Variations in radial anisotropy are different between continent and ocean. Strong anisotropy occurs at shallow depths (< 100 km) under the continents, with a secondary maximum at a depth of about 200 km. Maximum anisotropy under the oceans occurs at a depth of about 125 km, with no secondary maximum. Within the North American craton, the strongest anisotropy was found at the locations of fastest isotropic velocity.

Map of ray exit points

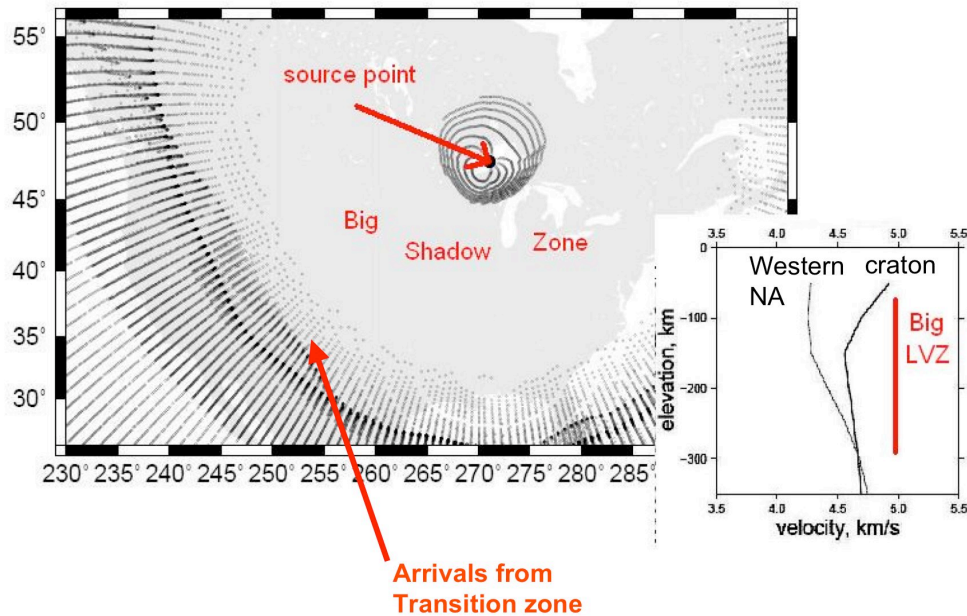


Figure 4. From a source point in Lake Superior, at the location of the EARLY RISE chemical explosions described below, rays are traced in a cratonic upper mantle model determined from surface waves. Each ray emerging at the surface of the model is plotted as a small dot. Much of North America is then in a shadow zone, i.e. without arrivals.

If compressional velocity V_p is approximately proportional to V_s of the type shown in Figure 4 then P -wave arrivals also would be prohibited throughout a vast region. We therefore did not use the Nettles and Dziewonski model directly, but rather constructed a model with only positive dV_p/dz that was broadly informed by their work. We started with the Nettles and Dziewonski 100-km depth Voigt-averaged shear velocities, computed the fractional perturbation from their mean value $\Delta V_s/V_s$, and took this quantity as a proxy for the overall thermo-chemical state of the uppermost mantle at a given latitude and longitude. We then modified the velocity of each 1/2 by 1/2 degree node in the 35–210 km range of our *AK135* model, as follows:

$$\begin{aligned}
 35 \text{ km: } & (1 - A + C \Delta V_s/V_s) * V_p(35 \text{ km}) \\
 120 \text{ km: } & (1 - A + C \Delta V_s/V_s) * V_p(120 \text{ km}) + B \\
 210 \text{ km: } & (1 - A + C \Delta V_s/V_s) * V_p(210 \text{ km}).
 \end{aligned}$$

The constants A and B represent a small overall adjustment of *ak135*'s mean uppermost mantle

velocity and velocity gradient. They were introduced because *ak135*, being a globally-averaged model, simply does not do an adequate job in predicting North America's mean travel time curve. We used $A = 0.01$ km/s, and $B = 0.15$ km/s. The constant C represents a scaling between V_s and V_p . We used $C = 0.56$, a value determined by comparing the tomographic reconstruction of North American Pn velocities at 50 km depth given by Phillips et al (2007), with corresponding values for the Nettles and Dziewonski Voigt-averaged shear velocities.

A flowchart outlining the above procedure is shown in Figure 5.

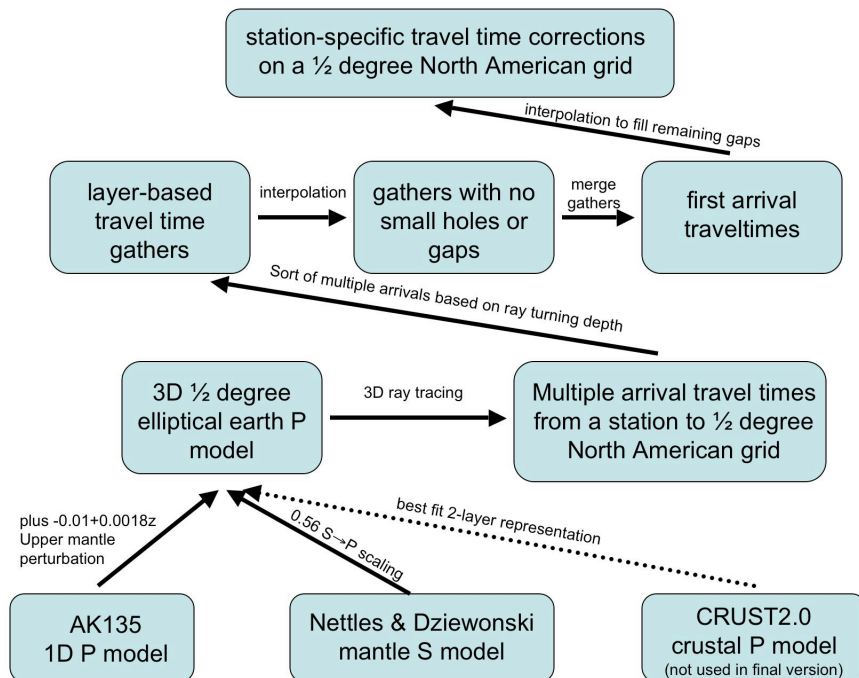


Figure 5. Flowchart for our procedures in developing the 3D model *NETTLESAK135G*.

The choice of parameters A , B , and C , was made in part to reproduce basic known features of anomalous P -wave arrival times, as documented for example by a dataset obtained from continental-scale observations recorded from the underground nuclear explosion GNOME. See Figure 6.

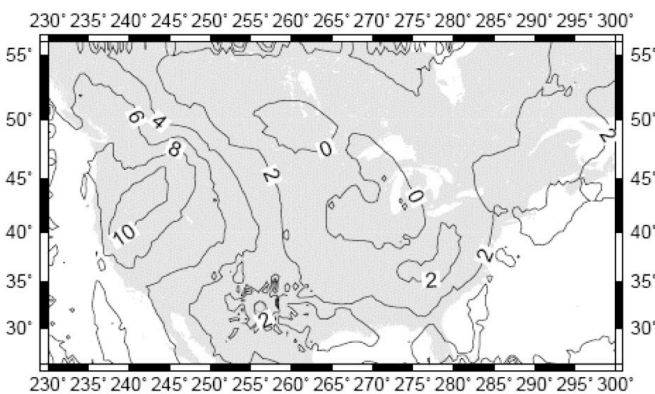
We tested the travel-time predictions of this 3D model against those observed for 5 underground nuclear explosions and the Early Rise series of large chemical explosions. Figure 7ab gives these results. (A description of the observational data for these events is given below. Most of these explosions took place in the 1960s. It is remarkable, that such an old dataset is still one of the most relevant sets of empirical travel time data for North America.) *NETTLESAK135G* reduces the observed travel time residuals by about 50% compared to those of *AK135*. For example, EARLY RISE travel times residuals are reduced from 2.93 s to 0.94 s.

CRUST2.0: Our *NETTLESAK135G* model has the same 35-km thick crust as our *AK135* model. However, we did examine the effect of replacing that crust with one based on the published Crust2.0 model. We constructed this model by starting with the published Crust2.0 velocity-depth

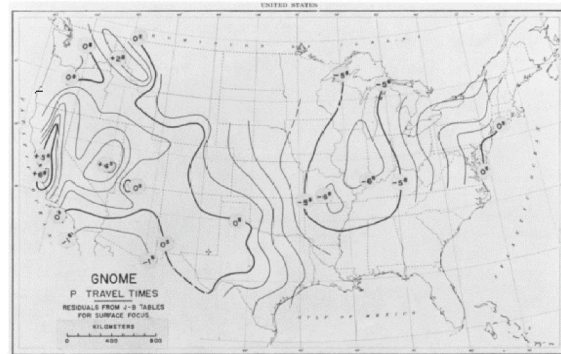
model (which typically has several constant velocity layers), and approximating it with a two constant-velocity-gradient layer model of the same overall thickness that ‘best-fits’ the travel times of the original model (out to the range of the predicted Pg – Pn crossover). In most cases, the r.m.s. travel-time difference between the original and approximated models are just a few milliseconds. However, an overall Earth model that incorporates this crust did not do significantly better than *NETTLESAK135G* in predicting PNE and Early Rise travel times. This result is probably not a reflection on the accuracy of Crust2.0, which may well be quite good. Instead, it probably reflects the fact that the effect of the crust on travel-time residuals is rather small (a few tenths of a second) compared to the effect of the mantle (a few seconds), at least for the region studied in this project (North America). Thus a small change in ray path induced by a heterogenous crustal structure might lead to a spurious change in the travel time of the mantle segment of the ray, whose size is comparable to the change of the travel time in the crust itself.

Example of “motivating the construction”

Nettles & Dziewonski (2007) Vs-Voigt at 50 km depth, scaled to V_p , and used to tweak velocity up & down uniformly throughout an ak135 lithosphere



Travel-time residuals predicted by model



Travel-time residuals observed for Gnome explosion

Figure 6. Motivation for our approach to modeling, by matching residuals. The residuals from the GNOME nuclear explosion (against a standard 1D model) are very substantially different in Eastern and Western North America. The final 3D earth model developed in this project, was designed to exhibit the same feature,

To summarize our work on development of a 3D model based mainly upon surface-wave studies: on the one hand, models of this type are limited by their low horizontal resolution (hundreds of kilometers) and by providing estimates of shear velocity but not compressional velocity. But on the

other hand, they have the virtue of having a uniform spatial resolution and are based on data (surface wave dispersion) that are only very weakly dependent on the location and origin time of the underlying earthquake sources. This near independence is relevant, for instance, in developing velocity models and/or travel-time models for earthquake location, because the problems associated with circularity-of-results (e.g. the same earthquakes both determining the model and being located by it) are avoided. In *NETTLESAK135G* we built such a model of North America and tested it against continental-scale travel times from five PNE's and the EARLY RISE series of chemical explosions. Travel-time residuals were reduced by 50 percent compared to the predictions of the radially-stratified model *AK135*, but some regionally coherent travel-time residuals remain, as can be seen in the middle column of subfigures in Figures 7ab, indicating that the 3D model derived from surface waves is capturing some, but not all, of the actual variability beneath the continents.

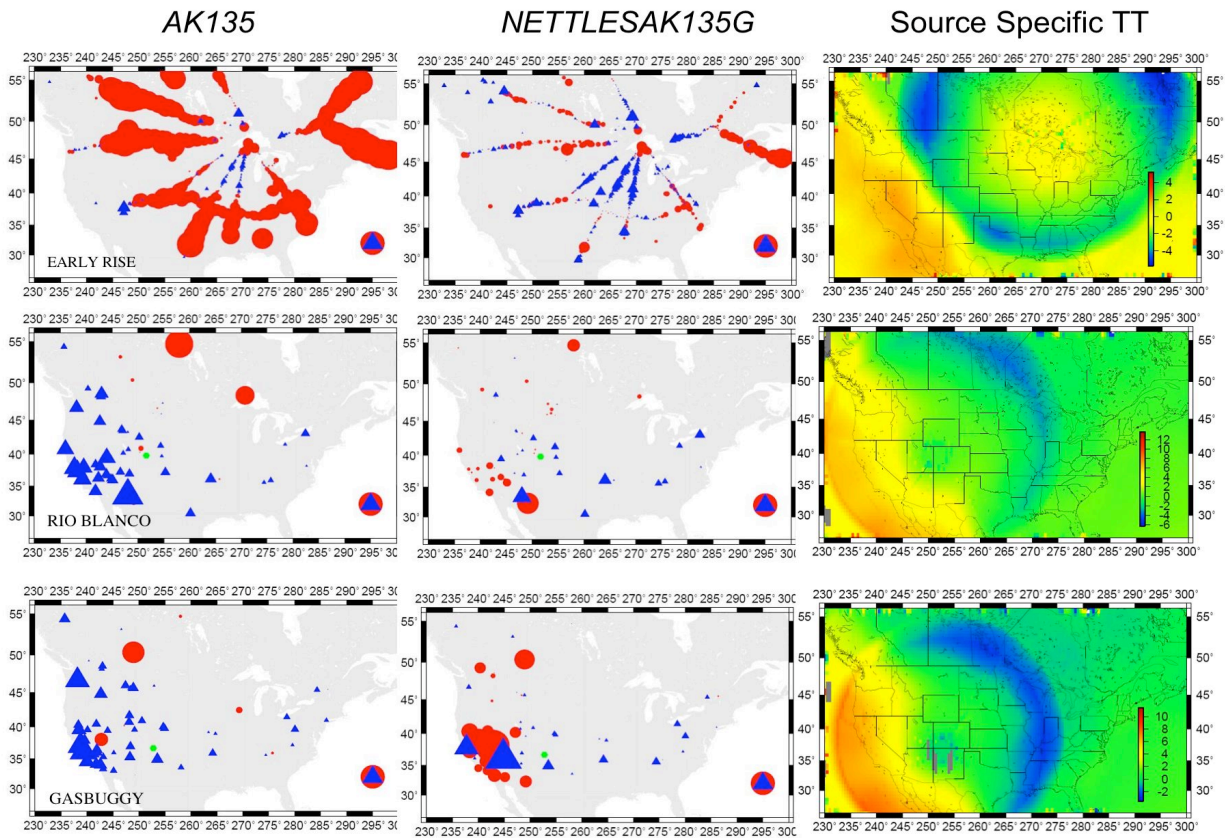


Figure 7a. Residuals (observed – calculated) of travel times for the EARLY RISE, RIO BLANCO, and GASBUGGY explosions (rows 1, 2, and 3), for the *AK135* and *NETTLESAK135G* Earth models (columns 1 and 2). The source location is given by a green dot in each subfigure. The final column shows the difference between travel times in the *NETTLESAK135G* and *AK135* Earth models, for each of these three source locations. In the left-hand six sub-Figures, the red circle and blue triangle in each bottom right corner denote ± 5 s residuals. A red residual indicates negative value, i.e. that an observed arrival is advanced (fast) compared to model prediction.

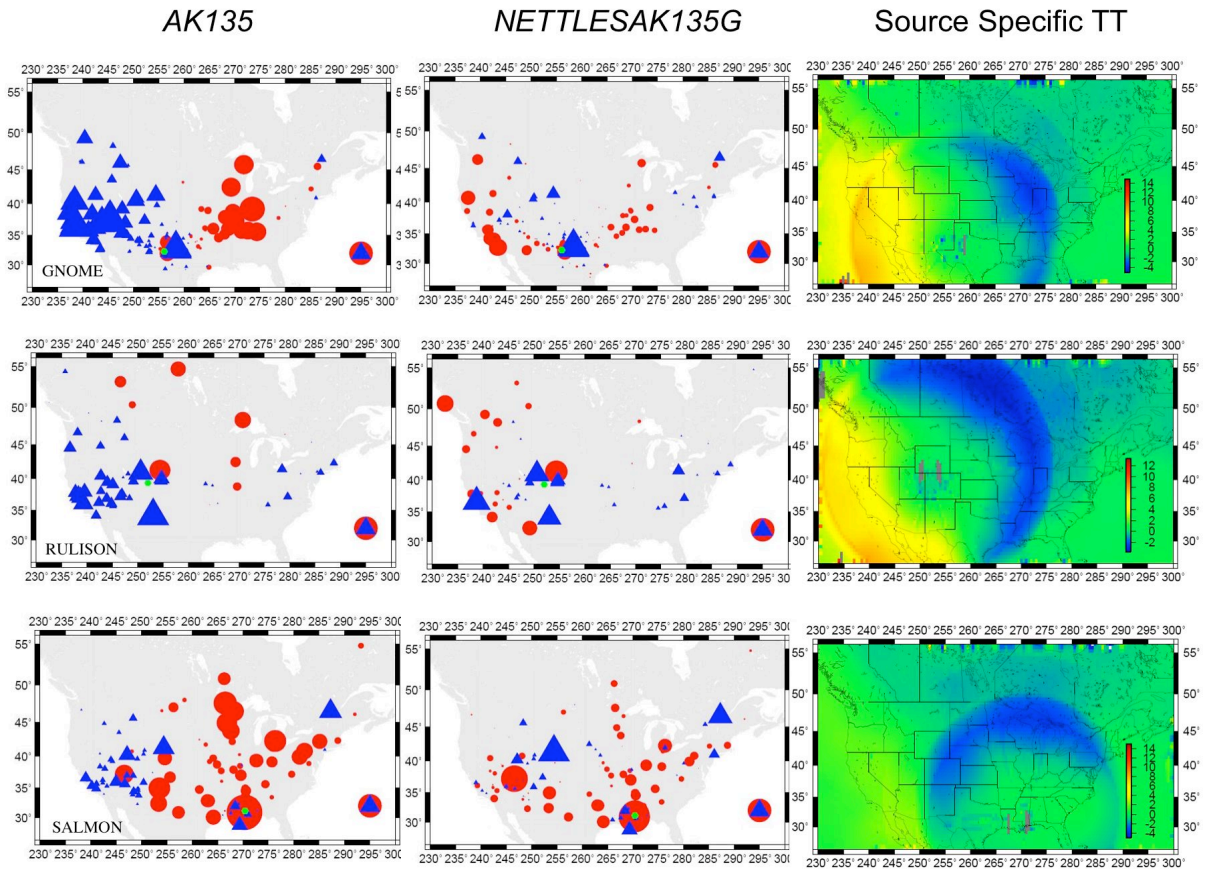


Figure 7b. Residuals (observed – calculated) of travel times for the GNOME, RULISON, and SALMON nuclear explosions (rows 1, 2, and 3), for the AK135 and NETTLESAK135G Earth models (columns 1 and 2). The final column shows the difference between travel times in the NETTLESAK135G and AK135 Earth models, for each of these three source locations. In the left-hand six sub-Figures, the red circle and blue triangle in each bottom right corner denote ± 5 s residuals. A red residual indicates a negative value, i.e. that an observed arrival is advanced (fast) compared to model prediction.

Empirical Travel Times from Explosions

The GNOME nuclear explosion of December 1961, conducted in a salt dome in New Mexico, though only of about 3 kilotons in yield, was pre-announced and numerous temporary stations were operated at many sites in North America to obtain seismic signals. The P_n arrivals in much of eastern North America were observed up to 6 seconds earlier than predicted by standard Earth models (such as Jeffreys-Bullen). From the special issue of the Bulletin of the Seismological Society of America for December 1962, we have scanned tables of station coordinates and the associated arrival times observed at these stations (Romney et al, 1962).

We have such empirical travel-time data for a somewhat smaller station set from a few additional nuclear explosions, namely for SALMON, RULISON, RIO BLANCO, and GASBUGGY. Table 1 gives parameters of the five nuclear explosions for which we obtained travel-time data.

These five events are highest quality, that is, GT0. Figure 8 shows the stations for which we have these empirical travel times. We acquired these data from ISC bulletins and special studies such as that by Romney et al (1962) for GNOME and Inge Lehmann (1969) for SALMON.

Name	Y	M	D	Time (GMT)	Y (kt)	DOB (m)	Lat. ° N	Long. ° E	El. (m)	depth (km)
GNOME	1961	12	10	19:00:00.00	3	361	32.264	-103.866	1013	0.36
SALMON	1964	10	22	16:00:00.00	5.3	828	31.142	-89.570	46	0.83
GASBUGGY	1967	12	10	19:30:00.14	29	1292	36.678	-107.209	2179	1.29
RULISON	1969	10	09	21:00:00.01	40	2568	39.356	-107.949	2469	2.57
RIO BLANCO 1	1973	05	17	16:00:00.12	33	1780	39.793	-108.368	2005	1.78
RIO BLANCO 2	1973	05	17	16:00:00.12	33	1899	39.793	-108.367	2005	1.90
RIO BLANCO 3	1973	05	17	16:00:00.12	33	2039	39.793	-108.368	2005	2.04
combine as RIO BLANCO	1973	05	17	16:00:00.12	100	1900	39.793	-108.367	2005	2

Table 1. Parameters of five underground nuclear explosions for which we have travel-time data at stations shown in Figure 8.

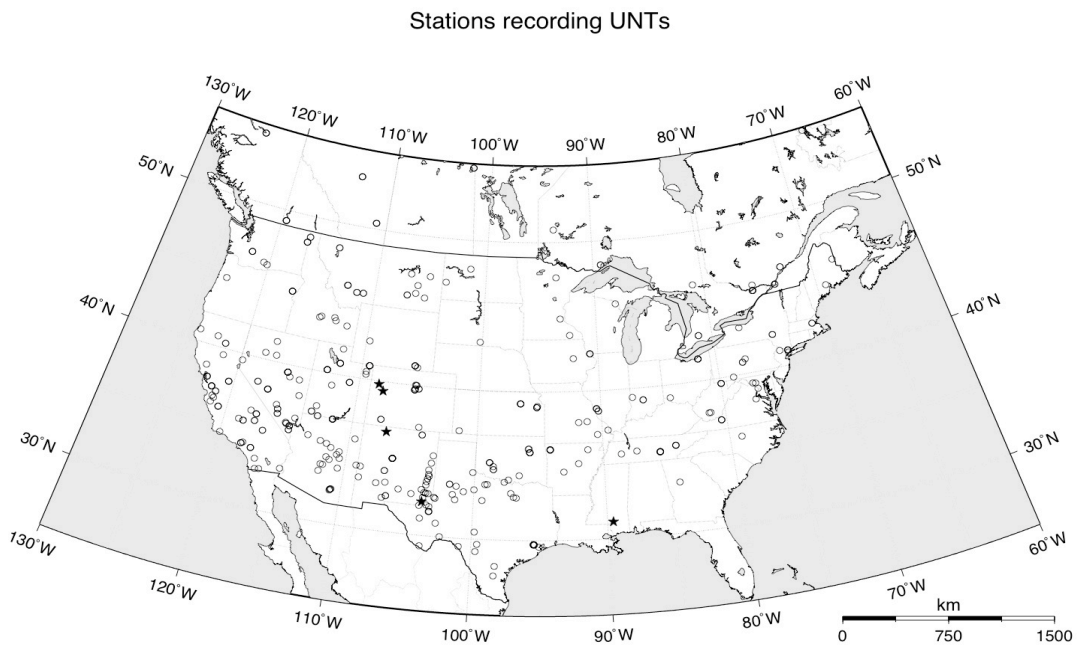


Figure 8. Stations for which we have travel times from five nuclear explosions (stars).

Another important set of empirical data is associated with the EARLY RISE project, which entailed 38 separate shots, all carried out during July 1966 by exploding about 5 tons of TNT equivalent for each shot, on the floor of Lake Superior in a depth of about 190m of water. Such an experiment probably would not be allowed today. Coupling into seismic signal was excellent, with numerous teleseismic detections. Four of the shots were somewhat more than 1 km from the centroid of all the shots. Removing these four, the centroid of the remaining 34 shots is (47.5506 degrees N, -88.9390 deg E) (at a depth of 190 meters). A map of these 34 shot locations is shown in Figure 9. These are GT1 events. The location of the EARLY RISE stations is apparent in the maps of residuals that can be seen in the top row of Figure 7a (first two sub-Figures).

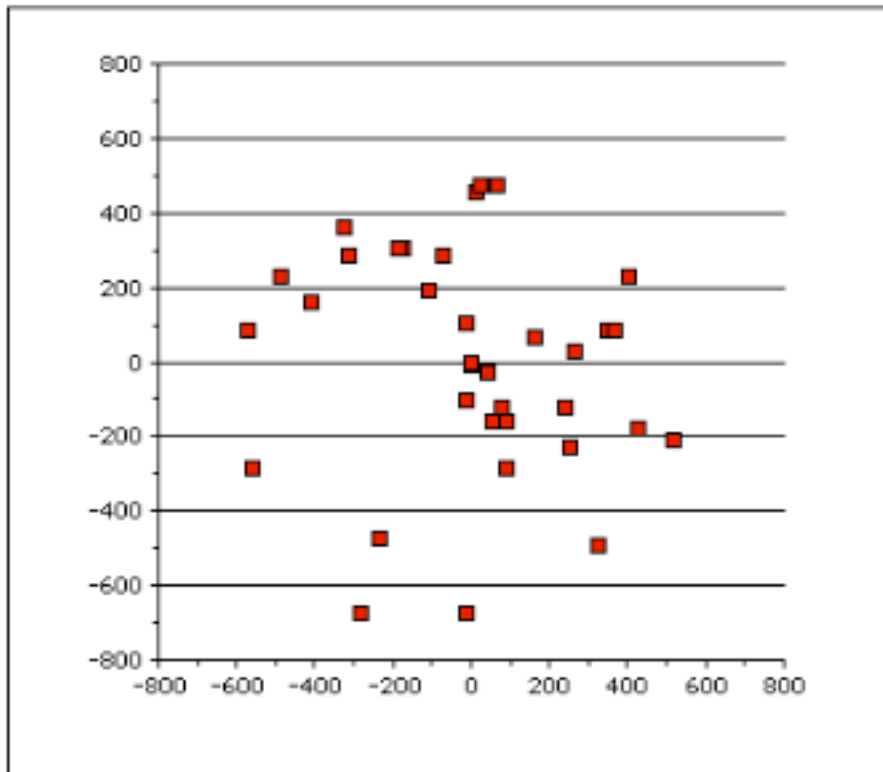


Figure 9. Map of 34 Early Rise shot locations, in meters with respect to their centroid at (47.5506 deg N, -88.9390 deg E) depth 190m (on the floor of Lake Superior), July 1966.

Numerous papers were written in the 1960s and 1970s, presenting and interpreting these data from EARLY RISE, in particular reporting the travel times as recorded for each shot at hundreds of different stations out to teleseismic distances. It turned out to be surprisingly difficult today to find an electronic copy of these travel times. About 15 people were contacted, who had participated in some aspect of this project, and initially none of these contacts was able to help. Just when we were about to give up this approach and to initiate a time-consuming effort to scan all of the old printed tables of reported travel times for these shots, we were able to obtain an electronic copy of relevant ascii files from Hans Thybo. But these still left out about a third of the available data, and for them we therefore did carry out the necessary work of scanning and optical character recognition applied to Tables in the paper by Iyer et al (1969) to complete the recovery of this data in usable form. The resulting dataset is likely to be a useful product of this NEHPR project.

Our selection of Ground Truth events, and the station set

Choice of Ground Truth Events

Our proposal to USGS listed 16 events for which we had confidence in the accuracy of hypocenter information, at the GT5 level. (GT5 is a measure of confidence in the epicenter value, not in the depth. Depths and origin times are typically less well known — unless constrained by waveform modeling — and their errors are correlated.)

Subsequently we added several more events, and did our relocation analysis using the 29 events listed in Table 2. In the end, the list included seven events of GT10 quality, i.e. not as good as we would have liked. But most of the events are of GT5 quality or better.

Reference events (as of March 2008)

#	Date year-mo-dy	Time hh:mm:ss	Lat. (N)	Long. (W)	h (km)	Mag mb(Lg)	Location, quality, comment and/or reference
1	1967-04-10	19:00:25.6	39.867	104.891	5	5.0	Rocky Mt. Arsenal, GT3 [1]
2	1967-08-09	13:25:06.2	39.871	104.901	5	5.3	Rocky Mt. Arsenal, GT3 [1]
3	1967-11-27	05:09:22.7	39.870	104.888	5	5.2	Rocky Mt. Arsenal, GT3 [1]
4	1994-01-16	00:42:43.60	40.375	76.034	0.5	4.0	Reading, PA, GT2, [2]
5	1994-01-16	01:49:16.80	40.371	76.067	0.5	4.6	Reading, PA, GT2, [2]
6	1995-02-03	15:26:12.9	41.5183	109.8083	4	5.1	Trona mine, WY, GT5, [3]
7	1997-10-24	08:35:17.8	31.1167	87.3833	4	5.1	Atmore, Alabama, GT5, [4]
8	1997-11-05	23:00:08.1	37.2580	117.847	0	4.1	CA-NV Border, GT10, [5]
9	1998-09-25	19:52:52.0	41.495	80.388	5	5.2	Pymatuning, PA, GT5, [6]
10	2000-01-01	11:22:58.21	46.8400	78.9250	12	5.1	Teminskaming, Que, GT5, [7]
11	2000-04-20	08:46:55.47	43.9493	74.2568	8	3.9	Saranac Lake, NY, GT5, [8]
12	2001-01-26	03:03:21.50	41.8720	80.7960	2	4.2	Ashtabula, OH, GT2, [9]
13	2001-05-04	06:42:12.64	35.0817	92.1930	6	4.4	Enolar, AR, GT5, [10]
14	2001-06-03	22:36:46.98	41.8698	80.7707	2	3.0	Ashtabula, OH, GT2, [9]
15	2001-09-04	12:45:53.22	37.155	104.642	5	4.0	Trinidad, CO, GT10, [11]
16	2001-09-05	10:52:07.50	37.132	104.704	3	4.6	Trinidad, CO, GT5, [11]
17	2001-09-21	19:10:59.67	37.121	104.706	3	3.4	Trinidad, CO, GT2, [11]
18	2002-04-20	10:50:47.15	44.5090	73.6750	11	5.3	Au Sable Forks, GT2, [12]
19	2002-05-24	23:46:00.04	44.5060	73.6740	12	3.1	Au Sable Forks, GT2, [12]
20	2002-06-05	20:17:37.00	52.850	74.354	4	4.5	Northern Quebec, GT10, [13]
21	2002-06-18	17:37:17.20	37.9920	87.7720	18	5.0	Caborn, Indiana, GT2, [14]
22	2002-11-03	20:41:56.91	42.7680	98.8960	8	4.3	Martin, NB, GT10, [15]
23	2002-11-11	23:39:29.72	32.4043	79.9363	9	4.2	South Carolina, GT10, [16]
24	2003-04-29	08:59:38.62	34.4710	85.6257	13	5.3	Fort Payne, AL, GT3, [17]
25	2003-04-30	04:56:22.0	35.940	89.920	23	4.0	Blytheville, AR, GT5, [18]
26	2003-05-25	07:32:33.39	43.098	101.747	20	4.4	South Dakota, GT10, [19]
27	2003-06-06	12:29:34.00	36.8750	89.0100	02	4.5	Bardwell, KY, GT1, [20]
28	2003-12-09	20:59:18.72	37.7753	78.0997	10	4.5	Central Virginia, GT10, [21]
29	2005-03-06	06:17:49.72	47.7511	69.7295	13	4.6	Riviere-du-Loup, Qc, GT5, [22]

Table 2. Earthquakes of GT quality, whose locations have been estimated in a variety of special studies, and for which we have empirical travel-time data. Numbers in square brackets in the final column refer to numbered comments and references below, in support of the quality (GT level) given in this same column.

We were guided in assigning the Ground Truth category, by the following table:

GT1-GT2	Located or re-located by employing JHD / double-difference event relocation methods using local seismographic network data with the distance to the nearest station less than focal depth. Regional + <i>local network data</i> .
GT3	Similar to GT2, but lack of high-quality map and other material.
GT5	Regional station data has a good coverage and the nearest station is located at a distance less than focal depth. Focal depth independently constrained by regional waveform modeling, or locally recorded aftershocks provide indirectly the range of epicentral area that include mainshock.
GT10	Located by regional seismographic network data with distance to the nearest station many times the focal depth. Station spacing on the order of 100 km or greater and relatively poor azimuthal coverage. However, focal depth is constrained by regional waveform modeling.

Table 3. Characteristics of the methods of event location used to assign GT quality.

We conclude this subsection on our choice of Ground Truth events by giving a list of numbered comments and numbered references, corresponding to the number in square brackets given in the last column of Table 2 for each GT event.

[1] Rocky Mountain Arsenal, Denver, Colorado. The list of large events in this series includes four events reported by two different agencies as

1967-04-10	19:00:25.6	39.900	104.800	5.0	4.8	USCGS
1967-08-09	13:25:06.2	39.900	104.700	5.0	5.3	USCGS
1967-11-27	05:09:22.7	40.000	104.700	5.0	5.2	USCGS
1967-11-27	05:35:00.7	39.900	104.700	5.0	4.4	USCGS
1967-04-10	19:00:25.5	39.930	104.680	5.0	4.9	ISC
1967-08-09	13:25:06.7	40.000	104.690	5.0	5.2	ISC
1967-11-27	05:09:23.4	40.010	104.760	5.0	5.1	ISC
1967-11-27	05:35:04.0	39.800	105.000	5.0		ISC

Three of these events were selected as reference events, because:

1) A local network was deployed around the Rocky Mountain Arsenal Well (an injection well) for earthquake monitoring.

2) These three largest events, included in Table 2, were well located by using local network data. Our three GT locations, are from a Science paper given as reference [1] below. The paper gives no coordinates, but a map with these epicenters. We compared the published map with a topographic map to determine the actual coordinates. (If the coordinates had been given in the paper, these events could be GT2. The ISC locations are quite poor and are of lower quality than USCGS locations, done prior to the existence of NEIC and its PDE product.)

- [2] A local portable seismic network was deployed for aftershocks. Foreshock #4 and the mainshock #5 were relocated by using JHD technique. Depth constrained by regional waveform modeling (Du et al. 2003, reference [8] below).
- [3] large location uncertainty due to large azimuthal gap (196 degree) and lack of close-by stations from the event (nearest station, distance =128 km).
- [4] Aftershocks were monitored by a 6-station local seismographic network deployed after the mainshock. Aftershock distribution is relatively clustered and GT5 is appropriate for the mainshock location. Depth constrained by regional waveform modeling (Du et al. 2003, [8]).
- [5] Calibration Event Bulletin (CEB), pIDC, GT10, quality is poorly known.
- [6] 12-station local seismographic network was deployed following the mainshock. However, the largest aftershocks had $M \sim 2$, and could not be used for mainshock relocation using JHD. Relocated mainshock epicenter is within about 5 km from the aftershock cluster. Depth constrained by waveform modeling (Maceira et al., 2000, [6]; Du et al. 2003, [8]).
- [7] Event located by CNSN (Canadian National Seismographic Network) using sparse regional data. Depth is constrained by regional waveform modeling (Du et al. 2003, [8]).
- [8] Depth is constrained by regional waveform modeling (Du et al. 2003, [8]) and the nearest station is closer than the focal depth.
- [9] local portable seismic network deployed for aftershocks, and the mainshock #12 was relocated by using JHD technique with earthquake #14 as the master event. Depth is constrained by regional waveform modeling (Du et al. 2003, [8]).
- [10] Located by CERI with dense seismic array in New Madrid seismic zone. Depth is constrained by regional waveform modeling R. Herrmann of St. Louis University and is posted at URL:
http://www.eas.slu.edu/Earthquake_Center/MECH.NA
- [11] A local portable seismic network was deployed for aftershocks by USGS, and the mainshock on Sept 05 has been relocated by using JHD technique with the smaller event on Sept 21 as the well-recorded master event (personal communication, Mark Meremonte, 2007). An earlier event on Sept 04 was not so near the mast event, and we assign it as GT10.
- [12] Local portable seismic network deployed for aftershocks by LDEO, and the mainshock #18 was relocated by using JHD technique with earthquake #19 as the master event. Depth is constrained by regional waveform modeling (Du et al. 2003, [8]).
- [13] Located by CNSN (Canadian National Seismic Network) relatively poorly located event, but depth is constrained by regional waveform modeling (Kim, 2002 unpublished material). This event was selected for its location in an aseismic part of northern Quebec.

- [14] Local portable seismic network deployed for aftershocks, and the mainshock #21 was located by regional P and S arrival times as well as by inspecting waveforms at a pair of nearby stations which recorded also an aftershock. Depth is constrained by regional waveform modeling (Kim, 2003, [14]).
- [15] Located by NEIC with relatively poor regional & local station coverage. Depth is constrained by regional waveform modeling (R. Herrmann of St. Louis University) and is posted at URL:
http://www.eas.slu.edu/Earthquake_Center/MECH.NA
- [16] Offshore event located by NEIC with relatively poor regional & local station coverage (S. Jaume, USC-Columbia, Personal comm., 2007). Depth is constrained by regional waveform modeling R. Herrmann of St. Louis University and is posted at URL:
http://www.eas.slu.edu/Earthquake_Center/MECH.NA
- [17] Local portable seismic network was deployed for aftershocks, and the mainshock #24 was located by regional P and S arrival times and its location is close to the aftershock zone. Depth is constrained by regional waveform modeling (Kim, 2003 unpublished material).
- [18] Located by the Center for Earthquake Research Information (CERI) with a dense seismographic array in the New Madrid seismic zone. Depth is constrained by regional waveform modeling (R. Herrmann of St. Louis University) and is posted at URL:
http://www.eas.slu.edu/Earthquake_Center/MECH.NA
- [19] Located by NEIC/USGS with relatively poor regional & local station coverage. Depth is constrained by regional waveform modeling Kim (2003 unpublished material) and R. Herrmann of St. Louis University and is posted at URL:
http://www.eas.slu.edu/Earthquake_Center/MECH.NA
- [20] Local portable seismic network was deployed for aftershocks, and mainshock #27 was relocated by using double-difference technique. Depth is constrained by regional waveform modeling (Horton et al. 2005, [20]).
- [21] Located by using P and S arrivals from relatively poor regional & local station coverage. Depth is constrained by regional waveform modeling Kim (2005).
- [22] Located by using a dense seismic array in Charlevoix seismic zone in Quebec. Depth is constrained by regional waveform modeling (Kim, 2005 unpublished material).

References for this section on our choice of Ground Truth events:

- [1] Healy, J.H., W. W. Rubey, D. T. Griggs, and C. B. Raleigh (1968). The Denver Earthquakes, *Science*, **161**, 27 September 1968, 1301–1310.
- [2] Seeber, L., J.G. Armbruster, W.-Y. Kim, N. Barstow and C. Scharnberger (1998). The 1994 Cacoosing Valley earthquakes near Reading, Pennsylvania: A shallow rupture triggered by quarry unloading, *J. Geophys. Res.*, **103**, 24505–24521.
Ammon, C. J., R. B. Herrmann, C. A. Langston, and H. Benz (1988). Faulting parameters of the January 16, 1994 Wyomissing Hills, Pennsylvania earthquakes, *Seism. Res. Lett.*, **69**, 261–269.
- [3] Pechmann, J. C., W. R. Walter, S. J. Nava, and W. J. Arabasz (1995). The February 3, 1995, ML 5.1 seismic event in the Trona mining district of southwestern Wyoming, *Seism. Res. Lett.* **66**, no. 3, 25–34.
- [4] Gomberg, J. and L. Wolf (1999). Possible cause for an improbable earthquake: The 1997 Mw 4.9 southern Alabama earthquake and hydrocarbon recovery, *Geology*, **27**, 367–370.
- [6] Armbruster, J., and fourteen others (1999). Preliminary results from the investigation of the Pymatuning earthquake of September 25, 1998, *Pennsylvania Geology*, **29**, no. 4, 2–14.
Maceira, M., C. J. Ammon, and R. B. Herrmann (2000). Faulting parameters of the September 25, 1998 Pymatuning, Pennsylvania earthquake, *Seism. Res. Lett.*, **71**, 742–752.
- [8] Du, Wen-xuan, Won-Young Kim, and Lynn R. Sykes (2003). Earthquake source parameters and state of stress for northeastern United States and southeastern Canada from analysis of regional seismograms, *Bull. Seism. Soc. Am.*, **93**, 1633–1648.
- [9] Seeber, L., J. Armbruster and W.-Y. Kim (2004). A fluid-injection triggered sequence in Ashtabula, OH: Implication for seismogenesis in stable continental regions, *Bull. Seism. Soc. Amer.*, **94**, 76–87.
- [11] Mark E. Meremonte, John C. Lahr, Arthur D. Frankel, James W. Dewey, Anthony J. Crone, Dee E. Overturf, David L. Carver, and W. Thomas Bice (2002). Investigation of an Earthquake Swarm near Trinidad, Colorado, August-October 2001, U.S. Geological Survey Open-File Report 02-0073.
- [12] Seeber, L., W.-Y. Kim, J. G. Armbruster, W.-X. Du, A. Lerner-Lam, and P. Friberg (2002). The 20 April 2002 Mw 5.0 earthquake near Au Sable Forks, Adirondacks, New York: A first glance at a new sequence, *Seism. Res. Lett.*, **73**, 480–489.
- [14] Kim, Won-Young (2003). The 18 June 2002 Caborn, Indiana earthquake: Reactivation of ancient rift in the Wabash Valley seismic zone?, *Bull. Seism. Soc. Am.*, **93**, 1633–1648, 2003.
- [20] Horton, S., Won-Young Kim and M. Withers (2005). The 6 June 2003 Bardwell, Kentucky earthquake sequence: Evidence for a locally perturbed stress field in the Mississippi Embayment, submitted to *Bull. Seism. Soc. Amer.*, **95**, 431–445.
- [21] Kim, W.-Y., and M. Chapman (2005). The 9 December 2003 central Virginia earthquake sequence: A Compound earthquake in the central Virginia seismic zone, *Bull. Seism. Soc. Am.*, **95**, 2428–2445.

Choice of stations

Our proposal to USGS listed 48 specific seismographic stations in North America which we would calibrate — that is, provide travel times for seismic waves used to locate events in the study region. Each station needs its own set of travel times as a function of source location.

Discussion with NEIC scientists during 2006 led to an increase from this original station list. First we moved to a set of 66 stations supplied to us by Dr. Jim Dewey in March (on grounds that these were the stations that provided the most phase picks for events worldwide, and that were therefore likely to be an appropriate station set for locating events in the eastern, central, and mountain states). Then in October 2006 we received coordinates for an additional set of US backbone stations. Merging these lists, our discussions with USGS personnel led us to focus our efforts on the following set of 80 stations:

AAM, ACSO, AGMN, AHID, AMTX, ANMO, BINY, BLA, BMO, BOZ, BRAL, BW06, CBKS, CBN, CCM, CCUT, CNNC, COWI, DGMT, DUG, DWPF, ECSD, EGMT, ELK, ERPA, EYMN, FCC, GLMI, GOGA, HDIL, HKT, HLID, HRV, HWUT, ISCO, JCT, JFWS, KSU1, KVTX, LAO, LBNH, LONY, LOZ, LRAL, LSCT, LTX, MCWV, MIAR, MNTX, MSO, MVCO, MYNC, NATX, NCB, NEW, NHSC, OXF, PAL, PKME, PLAL, RLMT, RSSD, SCHQ, SCIA, SDCO, SRU, SSPA, SWET, TUC, TXAR, TZTN, ULM, VBMS, WALA, WCI, WMOK, WUAZ, WVT, YKA, YKW3.

However, when we started in 2007 to work on the relocation of the 28 events for which we had good GT locations (Table 2), we found from the EDR (plus the ISC bulletin for the first two events) that 815 stations had at least one phase arrival time used for the location. Although many of

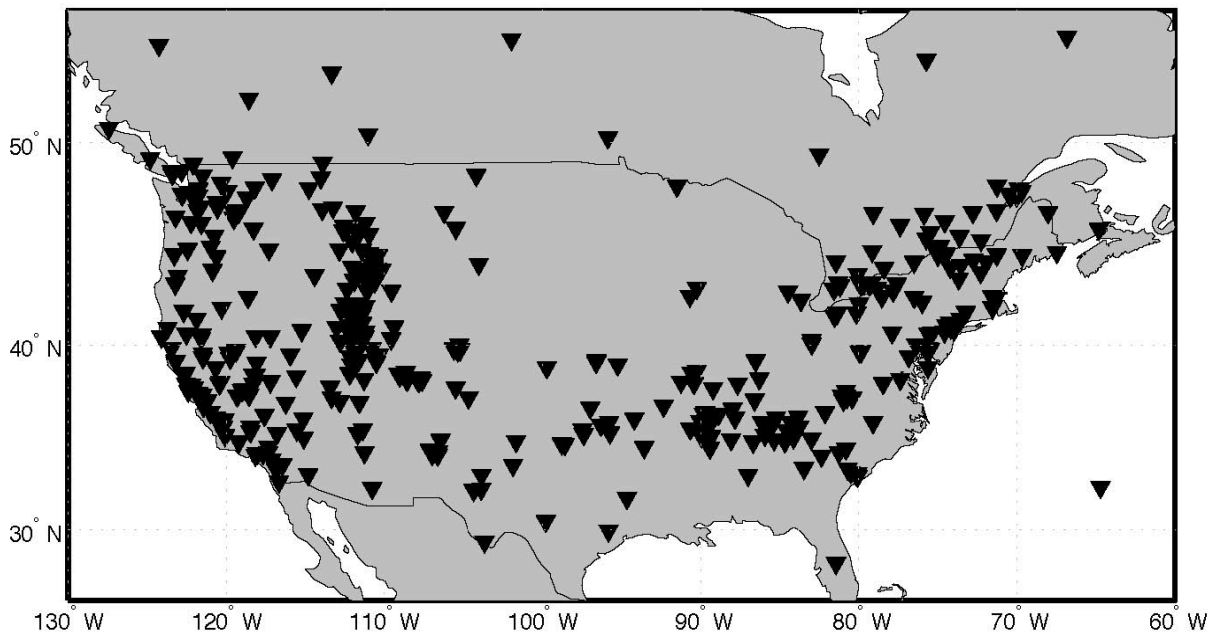


Figure 10. The 419 stations shown here contributed arrival time picks for the GT events in Table 2. We computed Source Specific Station Corrections for all of these stations — about ten times more stations than we originally envisaged. The bounding latitudes and longitudes of this Figure, are also the bounds of our 3D Earth model.

these were at teleseismic distances and our work has focussed on the interpretation of regional travel times, there were still a large number of regional stations. In the end, we computed regional *P*-wave travel time tables for the 429 stations (out of the 815) that are inside the bounding box for the 3D Earth model *NETTLESAK135G*, that is, the region bounded by latitudes 26N and 56N, and longitudes 130W and 60W. These 429 stations are shown in Figure 10.

Preliminary relocation estimates

We used the LOCSAT code to make location estimates in five different ways. We report these preliminary results here, noting that there is a practical limit to what we can accomplish in relocation studies at Lamont, without working closely with scientists at NEIC/USGS.

Our five different relocation estimates were conducted as follows:

- LOC0: LOCSAT locations without station corrections with *a priori* error set to EDR residuals using J-B travel times for events 1-28 and *ak135* for event 29.
- LOC1: locations without station corrections (same as LOC0) with *a priori* error set to one
- LOC2: locations without station corrections with *a priori* error set to EDR residuals in *ak135* travel time model
- LOC3: locations with station corrections with *a priori* error set to EDR residuals in *ak135* travel time model, with depth fixed to GT depth
- LOC4: locations with station corrections with *a priori* error set to EDR residuals in *ak135* travel time model, without depth fixed

Note that LOC0 results should be close to the PDE locations, since we were using the same phase picks as used, apparently, by the USGS in its EDR publication; and also were using the same travel-time model. (The USGS used the J-B travel times for its PDE locations up to the end of 2003, and subsequently switched to the *ak135* travel times.)

LOC1 results, to the extent they differ from those of LOC0, indicate events for which the location is sensitive to the weighting scheme.

LOC2 results should be similar to the relocations the USGS would obtain today, using the *ak135* model of travel times without Source Specific Station Corrections (SSSCs).

LOC3 results should show improvement over those of LOC2, to the extent that our SSSCs are appropriate (i.e., that our 3D Earth model, *NETTLESAK135G*, is good for producing *P*-wave travel times).

LOC4 results, compared to those of LOC3, indicate the effects on epicenter estimates due to uncertainty in depth.

In Table 4 we compare these five location estimates with the GT locations of Table 2, and with the published PDE locations.

#	PDE-GT	LOC0-PDE	LOC1-PDE	LOC2-GT	LOC3-GT	LOC4-GT	GAP1	GAP2
1	8.6033	9.8938	23.7238	17.1680	7.2087	6.7257	43	61
2	17.4917	12.0600	13.6596	23.7586	7.6046	4.8618	30	44
3	21.6002	4.8674	9.4440	24.3594	6.6584	5.8677	28	43
4	5.8026	0.3438	0.8390	7.4159	6.4921	5.9520	76	79
5	5.2175	1.1103	2.6495	6.7313	7.2421	6.8498	74	77
6	14.0725	0.8346	4.6534	12.1904	1.8580	2.1296	14	15
7	4.2281	8.8251	0.3620	7.9600	8.4368	10.0311	89	105
8	7.4617	0.3446	0.4188	13.4027	12.6051	12.6051	35	57
9	0.0000	1.4582	0.6870	3.0709	2.8077	3.4626	49	64
10	5.3497	1.0034	7.1031	1.7660	1.2990	1.9402	22	26
11	0.0000	0.3333	10.9738	5.8005	3.7976	4.5125	36	62
12	7.7909	1.8278	0.4293	7.2502	7.6742	7.7988	83	91
13	13.6463	2.9541	31.3093	7.1697	5.7782	6.7825	154	182
14	3.9016	1.4706	0.7458	9.4851	9.3598	9.2283	106	142
15	5.6157	4.9885	4.7134	3.6358	23.6802	24.5783	131	153
16	7.7381	0.5178	0.9017	8.2909	19.2992	21.9497	35	55
17	0.0000	2.2040	24.2885	6.7689	14.3001	14.0907	61	99
18	1.9594	5.9725	3.3276	6.0344	6.4003	6.0928	27	39
19	0.2360	4.2495	19.5542	11.8944	10.0014	5.9795	80	147
20	5.8339	3.0908	15.9145	6.2821	16.7683	14.8794	105	124
21	0.8955	0.4531	0.2831	4.4948	3.4257	2.3326	110	149
22	3.5699	10.2157	7.1539	11.1093	14.8652	13.4987	32	42
23	0.0000	22.0917	6.8144	10.1553	6.4647	8.7928	62	102
24	2.5694	2.5347	6.9543	12.9765	11.5868	11.7258	40	58
25	0.0000	2.6352	5.3284	8.0955	9.2628	5.8342	57	74
26	4.0171	11.4515	5.7854	8.0383	16.8351	15.5509	64	111
27	2.7317	0.3329	6.6019	4.6131	5.3553	5.4915	28	35
28	27.0696	1.7019	6.0169	14.2311	16.2998	18.5493	111	150
29	0.1112	1.3501	11.3110	1.3176	2.4138	2.2797	30	58
max	27.0696	22.0917	31.3093	24.3594	23.6802	24.5783	154	182
mean	6.1212	4.1764	7.9982	9.1540	9.1649	8.9784	62	84

Table 4. Our five different location estimates are compared with PDE and GT locations. All distances here are in km. GAP1 is the primary azimuthal gap. GAP2 is the so-called secondary azimuth gap (that is, the largest gap in azimuth that any one station closes).

In this final table of our preliminary results, the first column gives an event number, for easy comparison with the information on each event give in Table 2.

The second column gives the distance between the PDE and GT locations; it exceeds 20 km for two events. The third column compares the location given in the PDE, and our LOC0 locations — which are an attempt to reproduce the location in the PDE since we are using the same phase picks

and the same model of travel times that the USGS reportedly has used. While most of the distances between PDE and LOC0 locations are quite small (less than 5 km), there are a significant number of events for which these location estimates are more than 8 km apart, and one event for which they are more than 20 km apart. We will need to work with NEIC/USGS personnel to uncover the reason for these differences. It may be that the PDE is based upon use of only a subset of the stations for which travel times are reported in the EDR.

The next column compares LOC1 and PDE locations. To the extent this column agrees or disagrees with the LOC0 and PDE comparison, we are able to assess the degrees of independence or dependence of our weighting scheme on the location estimate. In most cases, it appears there is not much dependence on the weighting scheme, but for some specific events the dependence is quite large (e.g., ## 11, 13, 17, 19, 20).

The next three columns of Table 4 give differences between each of LOC2, LOC3, and LOC4, from the GT location. Perhaps the most appropriate comparison to make, to form some assessment of our project overall, is between the LOC3 – GT and LOC2 – GT columns. Thus LOC3 – GT indicates how good is our relocation based upon SSSCs for the 3D model *NETTLESAK135G*. And LOC3 – GT indicates how good is the relocation using something like USGS current procedures (*ak135* travel times). Figure 11 gives a comparison between these two columns.

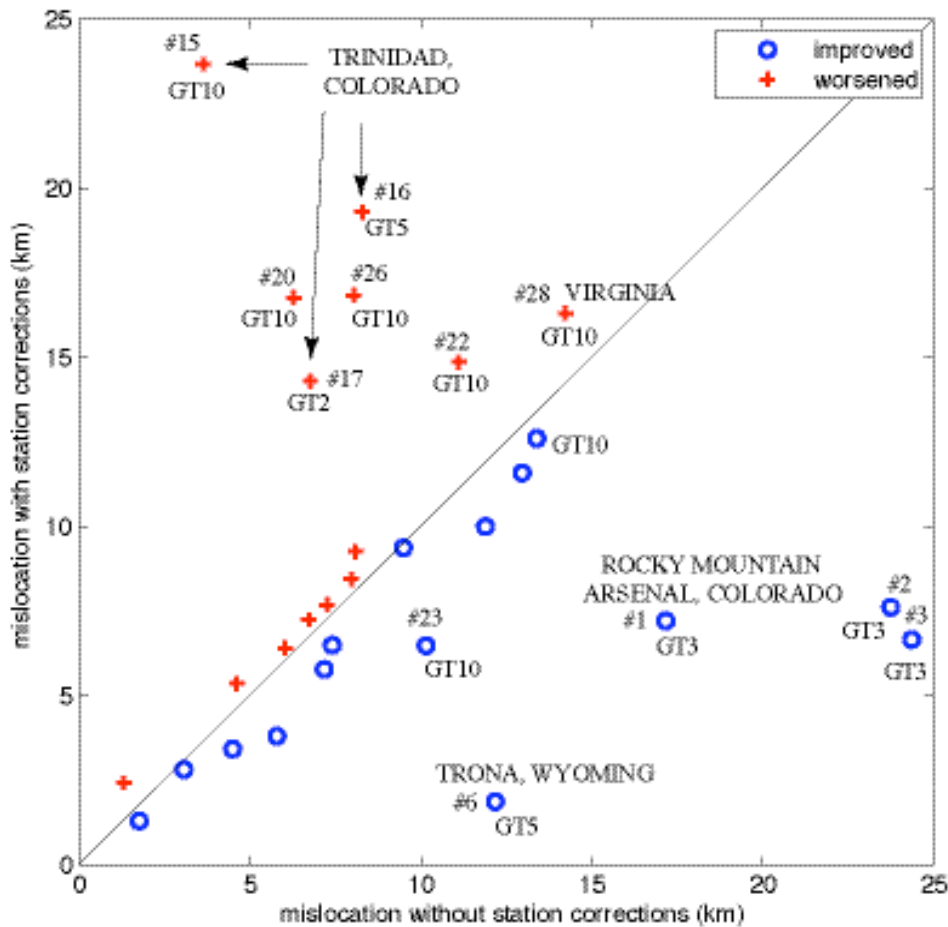


Figure 11. A comparison of mislocations, done with and without SSSCs.

If our project had been fully successful, all the events would show smaller mislocations using SSSCs, than without using SSSCs. That is, their vertical coordinate would be smaller than their horizontal coordinate and the points would all lie in the lower right part of the graph (blue circles). Indeed, several of the events show this feature. The four most notable events of this type are events ## 1, 2, 3, and 6, being the three Rocky Mountain Arsenal events, and the mine collapse in Trona, Wyoming. But the improvement in location estimates shown for these events when our SSSCs are used, appears to be countered by some “red” points for which the location is worsened when SSSCs are applied. The worst events of this type, are ## 15, 16, 17 (the three earthquakes at Trinidad, Colorado), and ## 20, 26, 22, and 28. It is of interest that these latter four events all have somewhat lower GT quality (they are all GT10), and so our estimate of their mislocation is itself somewhat uncertain. Concerning the Trinidad mislocations: the event #15 is the worst — and we note that it is a GT10 event, not as close to the master event as the main shock is, in the sequence (main shock is #16; master event is of quite small magnitude but was recorded on a local network).

There are many possible variations we could make, on the five relocation exercises we have undertaken in this preliminary evaluation. For example we could restrict travel times to all regional or all teleseismic, and we could eliminate all travel times that are associated with stations outside the latitude/longitude box shown in Figure 10 (i.e., eliminate all stations for which we did not use SSSCs). We did do this for the Central Virginia earthquake of December 2003 (for which the PDE location is quite poor). Although our relocations for this event all improve upon the PDE location, none of the mislocations are as small as we would like.

Our overall results as shown in Figure 11 may be summarized as follows:

There were six events that had been mislocated by more than 10 km, with respect to high-quality GT locations (GT5 or better). All six of their mislocations were reduced in our project when our SSSCs were applied. For four of these events (## 1, 2, 3, 6) it was a significant reduction. For two events (## 16, 17), both at Trinidad, Colorado, the mislocations were made worse by the use of our SSSCs.

Non-technical Summary

The goal of this project was to improve the accuracy of estimates of earthquake location for events in the easternmost 40 States of the U.S. plus parts of Arizona, Nevada, and Idaho. We developed a model of the travel times needed at each of 429 seismographic stations, to interpret the arrival times of signals detected at these stations. We use computer models of Earth structure, and also a special set of earthquakes and explosions, whose locations were accurately known, to obtain the model of travel times needed for these stations. We were able to improve locations estimates for several of the events in our study region, but some anomalies remain. In particular we had difficulty with a set of events in Colorado.

Presentations

We have had several interactions with USGS personnel on this project. In December 2007, Bill Menke presented a poster at the annual meeting of the American Geophysical Union, with the following abstract:

Abstract, December 2007 AGU meeting:

S11B-0565

Menke, W., Richards, P. G., Kim, W., Waldhauser, F., and Schaff, D.

Testing Models of North American Seismic Velocity Structure With Traveltimes From Well-Validated Sources

Surface wave tomography has provided 3D models of the seismic structure of the continents, down to depths of several hundred kilometers (e.g. Van der Lee and Nolet, 1997; Nettles and Dziewonski, 2008). On the one hand, these models are limited by their low horizontal resolution (hundreds of kilometers) and by providing estimates of shear velocity but not compressional velocity. On the other hand, they have the virtue of having a uniform spatial resolution and are based on data (surface wave dispersion) that are only very weakly dependent on the location and origin time of the underlying earthquake sources. This near independence is relevant, for instance, in developing velocity models and/or traveltime models for earthquake location, because the problems associated with circularity-of-results (e.g. the same earthquakes both determining the model and being located by it) are avoided. We discuss the conceptual and practical problems associated with using surface wave results to calculate continental-scale traveltimes and to locate earthquakes. We build such a model of North America and test it against continental-scale traveltimes from five PNE's and the Early Rise series of chemical explosions. Traveltime residuals are reduced by 50 percent compared to the predictions of a radially-stratified model, but some regionally coherent traveltime residuals remain, indicating that the 3D model derived from surface waves is capturing some, but not all, of the actual variability beneath the continents.

In June 2007, Bill Menke and Paul Richards participated in a workshop held in Berkeley, California, organized by the Lawrence Livermore National Laboratory, on the general subject of research into 3D Earth structure. A goal of the workshop was to identify practical uses of improved 3D modeling efforts, as well as to characterize current research and how it may contribute to practical results in monitoring explosions and managing seismic hazard. Menke's graphics prepared for this meeting are available at the following URL:

http://www.ldeo.columbia.edu/users/menke/talks/llnl3d/menke_llnl3d.ppt

The following report has been prepared, as a result of this Livermore-sponsored workshop:

Tarabay Antoun, Dave Harris, Thorne Lay, Stephen C. Myers, Michael E. Pasyanos, Paul G. Richards, Arthur Rodgers, William R. Walter, and John J. Zucca, On the use of three-dimensional Earth models to improve nuclear explosion monitoring and ground motion hazard assessment, in preparation for Seismological Research Letters, 16-page draft, November 7, 2007.

Datasets generated in this project

The data sets developed in this project are all derived from openly available data (waveforms, travel times, meta-data), much of it archived at the Data Management Center of the IRIS Consortium. Other input data have been provided to us by USGS/NEIC.

All our data products are available on request to the Principal Investigator as follows:
Paul G. Richards (845) 365 8389 richards@LDEO.columbia.edu

Our data sets include:

Travel times from 5 nuclear explosions and EARLY RISE chemical explosions, to stations in North America.

Source-Specific Station Corrections for the 429 stations shown in Figure 10. These corrections are for the first arriving *P*-wave, from points on the Earth's surface, in a half-degree by half-degree grid, for each station. The corrections are with respect to the *AK135* Earth model (essentially *ak135*, with ellipticity corrections), so that our travel time model is that for *AK135*, plus the SSSCs using interpolation within the grid to get the theoretical travel time for a candidate source location to a particular station out of the 429 we studied.

Travel times used to relocate the events listed in Table 2, and output from different LOCSAT relocations for these 29 events.

A large ascii text file specifying the Earth model *NETTLESAK135G*. [The files specify the velocity at the node points and the way in which triangles are constructed from those node points. In Menke's code, Earth structure as specified as "warped layers." That is, regardless of the (latitude, longitude) of a vertical (radial) column along which velocity is sampled, the same number of layers (spheroidal shells) are encountered; but their thicknesses, and top and bottom velocities, may differ from place to place. The model is specified along vertical columns that can be arbitrarily located in (latitude, longitude). All columns must have the same number of layers. First order jumps are allowed across layers. The user specifies a triangular (as distinct from tetrahedral) tessellation of the columns, which subdivide the model into a series of volumes with triangular cross section, and each volume is itself subdivided by the layers. It has six vertices, three on the top and three on the bottom. This fundamental volume with triangular cross section (bounded top/bottom by layer boundaries and on the sides by the triangular tessellation) is then divided into 8 tetrahedra by adding a seventh internal node at its center. There is a rule for computing the position/velocity of the internal node and its corresponding velocity.]

Final Comments

A central issue in this project, has been whether mislocations are due primarily to inaccuracies in the phase pick data, or to inaccuracies in the travel-time model used to interpret arrival times. In this regard, it is of interest that a set of mislocated events — namely the three in the Trinidad, Colorado, sequence — exhibited a quite good consistency of residuals at common stations. This is an indication that phase picks are not the problem. Our travel time model, based upon a 3D velocity model of the crust and upper mantle, gave significant reduction of residuals for a set of very high quality travel times from GT0 and GT1 explosion sources. The SSSCs generated from this model, when used to relocate our GT5 or higher-quality events, led to significantly reduced mislocations for four cases where the mislocations were quite large; and it increased the mislocation significantly for two events (in the Trinidad, Colorado, sequence).

We used about ten times more stations in this project, than we expected to. But we were not able to work with very many GT events. With a greater number of events, we could have modified the travel-time model by kriging with empirical travel-time data.

References

- Iyer, H.M., L.C. Pakiser, D.J. Stuart and D.H. Warren, Project Early Rise: Seismic probing of the upper mantle, *J. Geophys. Res.*, **74**, 4409–4441, 1969.
- Kennett, B.L.N. Engdahl, E.R. and Buland R., Constraints on seismic velocities in the Earth from travel times, *Geophysical J. International*, **122**, 108–124, 1995.
- Lehmann, I., Travel times and amplitudes of the Salmon nuclear explosion, *Bulletin of the Seismological Society of America*, **59**, 959–966, 1969.
- Menke, W., Case studies of seismic tomography and earthquake location in a regional context, in *Seismic Earth: Array Analysis of Broadband Seismograms*, Alan Levander and Guust Nolet, Eds., Geophysical Monograph Series 157. American Geophysical Union, 7–36, 2005.
- Nettles, M.K, *Anisotropic velocity structure of the mantle beneath North America*, PhD Thesis, Harvard University, 2005.
- Nettles, M., and A. M. Dziewonski, Radially anisotropic shear-velocity structure of the upper mantle beneath North America, *J. Geophys. Res.*, in press, 2008.
- Phillips, W.S., Begnaud, M.L., Rowe, C.A., Steck, L.K., Myers, S.C., Pasyanos, M.E., *Pn tomography with lateral variations of the upper mantle gradient*, *Annual Meeting Abstracts*, Seismological Society of America, 2007.
- Romney, C., B.G. Brooks, R.H. Mansfield, D.S. Carder, J.N. Jordan, and D.W. Gordon, Travel times and amplitudes of principal body phases recorded from GNOME, *Bulletin of the Seismological Society of America*, **52**, 1057–1074, 1962.